Electronic Supporting Information

The supporting information describes the calculation of the coefficient of linear thermal expansion, experimental data for single crystal structures obtained from crystal C, Hirshfeld surfaces and fingerprint plots calculated from the room temperature structure (crystal A), Le Bail fitting information, elemental analysis, TG-DTA analysis, and magnetic susceptibility versus temperature.

Calculation of thermal expansion coefficients

Cell parameters are plotted in Figure S1 along with a smoothened graph (red curves in Figure S1). Smoothening of the data is necessary in order to get meaningful expansion coefficients, since these depend on the derivative of the cell parameters. For smoothening an adjacent averaging method has been used. The difference between the smoothened curve and the true data has been included in the esd's.

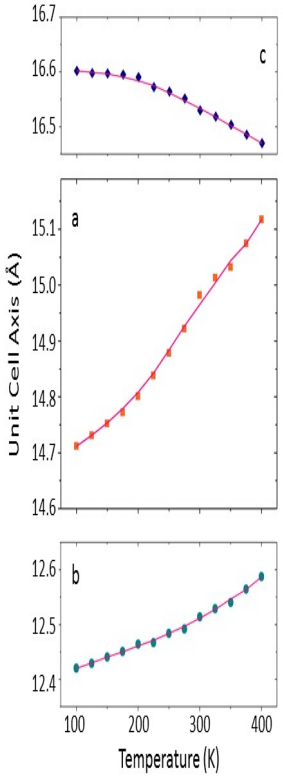

Figure S1. Unit cell axes (symbols) and smoothed curve (red lines).

The smoothened curve was differentiated and normalized to the experimental cell parameter value, *l*, at each temperature point. The expression αL=1l·∂l∂TP was used to calculate the linear thermal expansion coefficients shown in Figure 4.

Table 1 **Table S1 Experimental details for crystal C**

For all structures: M_r = 373.22, orthorhombic, *Pbca*, *Z* = 8, and the chemical formula is $C_9H_3MnO_6 \cdot C_6H_{11}N_2$. Experiments were carried out with Mo *K*α radiation using a SuperNova, Single source at offset, Atlas diffractometer. Absorption was corrected for by multi-scan methods, *CrysAlis PRO*, Agilent Technologies, Version 1.171.35.8 (release 07-03-2011 CrysAlis171 .NET) (compiled Mar 7 2011,18:06:32) Empirical absorption correction using spherical harmonics, implemented in SCALE3 ABSPACK scaling algorithm was applied. H-atom parameters were constrained.

	c100k	c160k	c220k	c280k
Crystal data				
Temperature (K)	100	160	220	280
a, *b*, *c* (Å)	14.6452 (4), 12.3672 (4), 16.6648 (5)	14.7079 (5), 12.3931 (4), 16.6458 (5)	14.7960 (5), 12.4275 (4), 16.6266 (5)	14.8837 (6), 12.4554 (5), 16.6018 (5)
V (Å^3)	3018.33 (16)	3034.14 (17)	3057.26 (18)	3077.69 (19)
μ (mm^{-1})	0.91	0.91	0.90	0.89
Crystal size (mm)	0.15 × 0.11 × 0.07	0.15 × 0.11 × 0.07	0.15 × 0.11 × 0.07	0.15 × 0.11 × 0.07
Data collection				
T_{min}, T_{max}	0.977, 1.000	0.974, 1.000	0.985, 1.000	0.981, 1.000
No. of measured, independent and observed [$I > 2\sigma(I)$] reflections	10796, 3611, 2412	10847, 3632, 2276	10927, 3673, 2208	11023, 3700, 2103
R_{int}	0.061	0.064	0.066	0.069
$(\sin \theta/\lambda)_{max}$ (Å^{-1})	0.689	0.689	0.692	0.689
Refinement				
$R[F^2 > 2\sigma(F^2)]$, $wR(F^2)$, *S*	0.055, 0.117, 1.07	0.066, 0.163, 1.05	0.066, 0.152, 1.05	0.074, 0.193, 1.03
No. of reflections	3611	3632	3673	3700
No. of parameters	254	212	212	210
No. of restraints	308	282	275	284

$\Delta\rho_{max}$, $\Delta\rho_{min}$ (e Å^{-3})	0.57, –0.57	0.88, –0.61	0.91, –0.63	0.86, –0.64

	c300k	c320k	c340k
Crystal data			
Temperature (K)	300	320	340
a, *b*, *c* (Å)	14.9204 (6), 12.4737 (5), 16.5884 (6)	14.9773 (6), 12.5017 (5), 16.5629 (6)	15.0401 (7), 12.5366 (5), 16.5320 (6)
V (Å^3)	3087.3 (2)	3101.3 (2)	3117.1 (2)
μ (mm^{-1})	0.89	0.89	0.88
Crystal size (mm)	0.15 × 0.11 × 0.07	0.15 × 0.11 × 0.07	0.15 × 0.11 × 0.07
Data collection			
T_{min}, T_{max}	0.980, 1.000	0.982, 1.000	0.979, 1.000
No. of measured, independent and observed [$I > 2\sigma(I)$] reflections	11042, 3708, 2054	11091, 3720, 2006	11134, 3747, 1947
R_{int}	0.071	0.071	0.073
$(\sin\theta/\lambda)_{max}$ (Å^{-1})	0.691	0.691	0.690
Refinement			
$R[F^2 > 2\sigma(F^2)]$, $wR(F^2)$, S	0.066, 0.166, 1.03	0.073, 0.200, 1.02	0.070, 0.193, 1.03
No. of reflections	3708	3720	3747
No. of parameters	213	212	213
No. of restraints	283	287	288
$\Delta\rho_{max}$, $\Delta\rho_{min}$ (e Å^{-3})	0.71, –0.65	0.79, –0.56	0.56, –0.53

Computer programs: *CrysAlis PRO*, Agilent Technologies, Version 1.171.35.8 (release 07-03-2011 CrysAlis171 .NET) (compiled Mar 7 2011,18:06:32), *SHELXL*, G.M. Sheldrick, Acta Cryst. (2008). A64, 112-122, O. V. Dolomanov, L. J. Bourhis, R. J. Gildea, J. A. K. Howard and H. Puschmann, OLEX2: a complete structure solution, refinement and analysis program. J. Appl. Cryst. (2009). 42, 339-341.

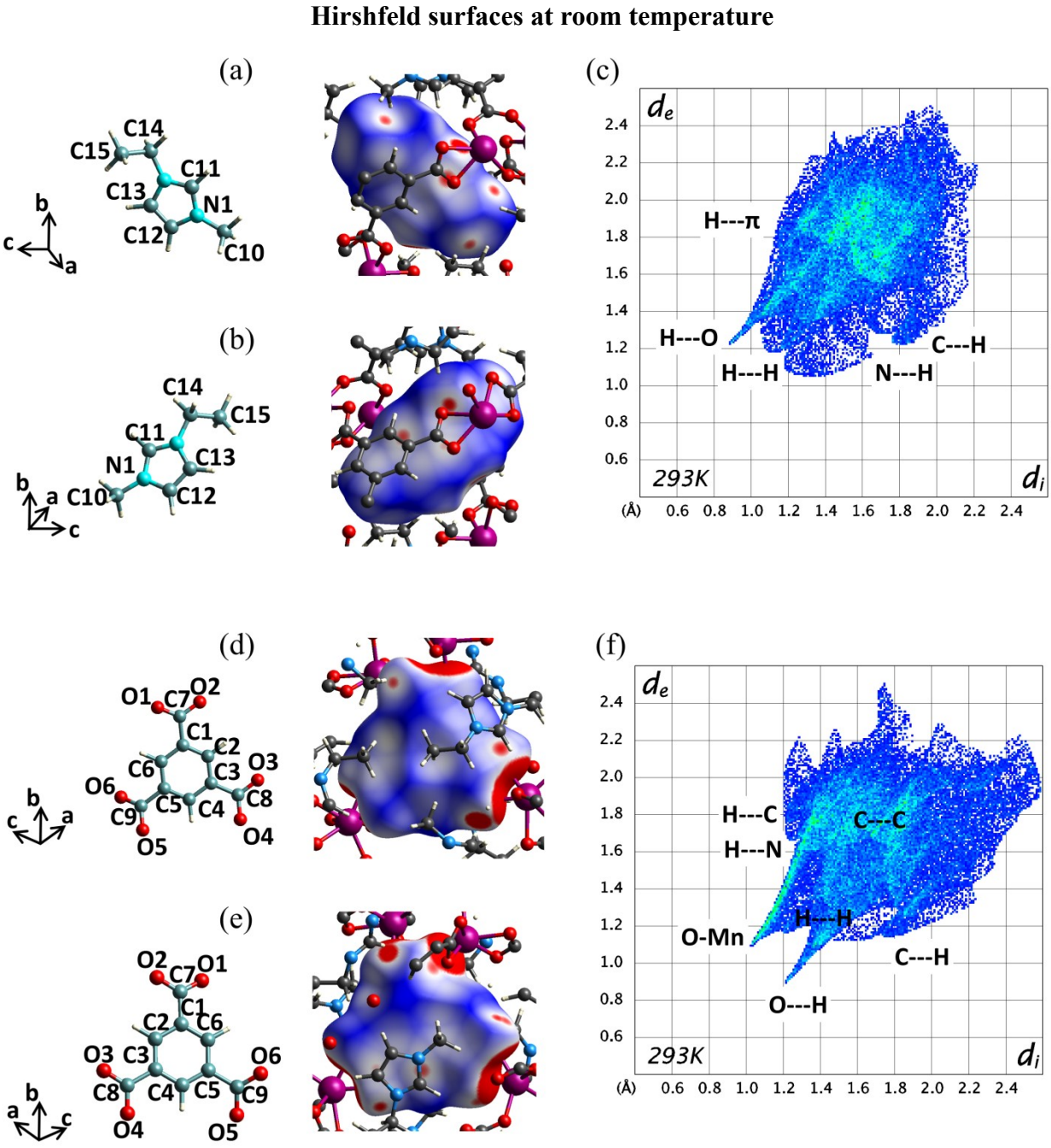

Figure S2. (a) and (b) Hirshfeld surfaces (293 K) with d_{norm} (range -0.1 – 1.0) of the $EMIM^+$ cation; (c) fingerprint plot of the $EMIM^+$ Hirshfeld surface showing two "spikes", the large one is H---O hydrogen bonds, the small one is H---H contacts; (d) and (e) Hirshfeld surfaces with d_{norm} of the BTC ligand; (f) fingerprint plot of the BTC ligand showing two spikes, one is the O---H hydrogen bonds, the other is the regular bond to Mn.

LeBail-fitting of unit cell dimensions

High resolution powder X-ray diffraction was obtained at the synchrotron facility SPring-8 in Japan. The 100K data is shown in Figure S3, and the fit parameters are listed for all temperatures in Tables S2 and S3.

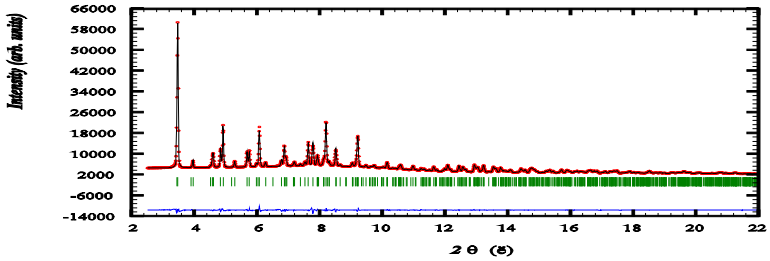

Figure S3. 100K powder X-ray diffraction data (red), the fit (black), peak positions (green) and difference plot (blue).

Table S2. Bragg-R values, fitted zero point and fitted unit cell parameters.

T (K)	Bragg-R (%)	Zero	a (Å)	b (Å)	c (Å)	V (Å^3)
100	0.0665	-0.000312(103)	14.7099(1)	12.4190(2)	16.6001(2)	3032
125	0.0954	-0.00352(9)	14.7297(1)	12.4274(2)	16.5993(2)	3038
150	0.0709	-0.0055(1)	14.7523(2)	12.4410(2)	16.5973(3)	3046
175	0.124	-0.0006(1)	14.7704(1)	12.4497(2)	16.5958(2)	3052
200	0.031	-0.0051(1)	14.8030(2)	12.4678(2)	16.5916(2)	3062
225	0.0282	-0.0003(1)	14.8450(2)	12.4832(2)	16.5804(3)	3073
250	0.0615	-0.0108(1)	14.8797(2)	12.4832(2)	16.5697(3)	3078

275	0.0434	-0.0081(1)	14.9215(2)	12.4924(2)	16.5553(3)	3086
300	0.0748	-0.0144(1)	14.9823(2)	12.5160(2)	16.5392(2)	3101
325	0.0359	-0.0117(1)	15.0120(2)	12.5279(2)	16.5190(2)	3106
350	0.0413	-0.0087(1)	15.0313(2)	12.5389(2)	16.5035(2)	3110
375	0.0466	-0.00717(1)	15.0740(1)	12.5623(2)	16.4828(2)	3121
400	0.0419	-0.00607(1)	15.1190(2)	12.5866(2)	16.4680(2)	3134

Table S3. Fitted gaussian and lorentzian parameters.

T (K)	**U**	**V**	**W**	**X**	**Y**
100	-0.15(1)	0.0385(1)	-0.00030(4)	0.047(8)	0.0110(4)
125	-0.12(1)	0.027(1)	0.00004(4)	0.129(8)	0.009(4)
150	-0.12(1)	0.030(1)	0.00295(5)	0.0005(1)	0.0121(4)
175	0.068(8)	0.019(1)	0.00028(4)	0.00140(7)	0.0136(4)
200	-0.003(9)	0.009(1)	0.00055(5)	0(0)	0.0145(5)
225	0.053(1)	-0.001(1)	0.00094(5)	0.00003(53)	0.0128(5)
250	0.05(1)	-0.0008(14)	0.00098(5)	0.0001(11)	0.0121(5)
275	0.029(9)	-0.003(1)	0.00104(5)	0.072(9)	0.0102(5)
300	-0.004(9)	0.003(1)	0.00093(5)	0.051(9)	0.0100(5)
325	0.042(9)	-0.006(1)	0.00116(5)	0.131(9)	0.0083(4)
350	0.031(9)	-0.006(1)	0.00118(4)	0.128(8)	0.0086(4)
375	0.14(1)	-0.014(1)	0.00140(4)	0.032(8)	0.012(4)
400	0.11(1)	-0.016(1)	0.00140(5)	0.174(9)	0.0096(4)

Elemental analysis (batch 1)

Table 4. Elemental analysis with X-ray fluorescence spectroscopy. Only the three major constituents are shown and C, N, O and H were not determined by this method.

Element	Concentration ww %	Error ww%
Mn	15.74	0.01
Br	2.02	0.002
Fe	0.0484	0.0012

TG-DTA

Thermo-gravimetric data shows a small gradual mass loss from 50-150°C which is caused by the evaporation of absorbed species from the surfaces of the particles. There is a pronounced step around 240-300°C where a total mass loss of 13.78% occurs (Figure S4) and the DTA curve shows an endothermal step as well. The 13.78% loss includes both the initial evaporation and the first breakdown, which amounts to 10-11% of the initial mass. The 10% correspond to the loss of the methyl and ethyl groups of the EMIM cations in the channels (combined weight 44 g/mol is 11.8w%). In the range 300-400°C there is a gradual weight loss, and above 400°C a major breakdown sets in removing additional 47.6% of the initial mass.

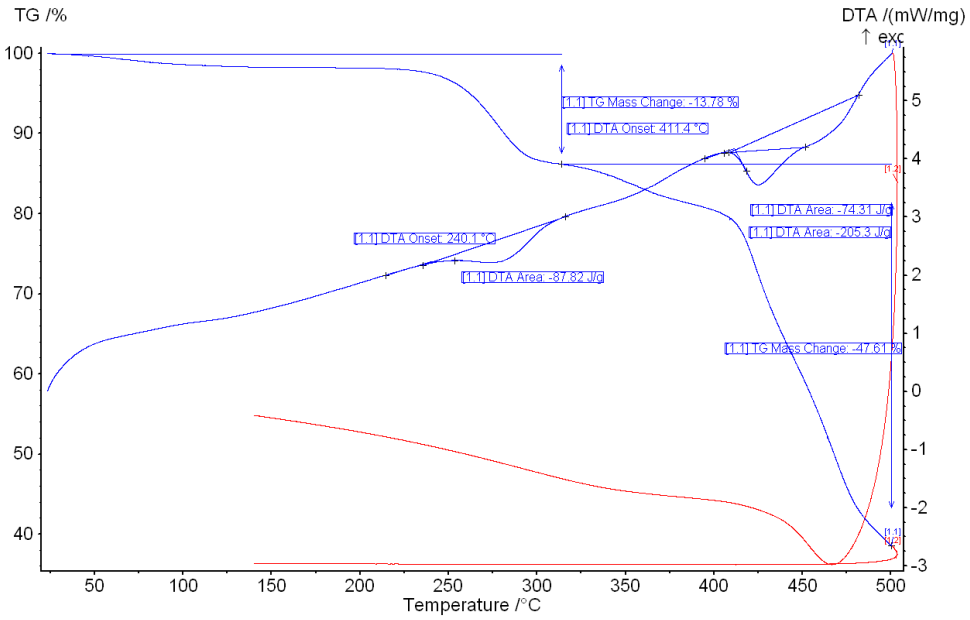

Figure S4. TG-DTA data showing a structural breakdown at 240°C (14 w%), and additional breakdowns from 400°C.

Magnetic data

The magnetization shows a local maximum at 6 K, indicating antiferromagnetic ordering at low temperature (Figure S5).

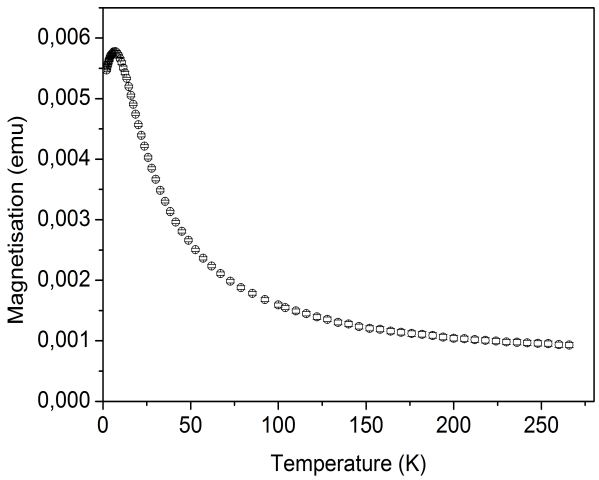

Figure S5. Magnetisation raw data versus temperature.

Though the powder data does not reveal any significant impurities, the single crystals of batch 1 contained a minor impurity (around 1 %) of an unknown substance. Therefore, fitting of the magnetic data to the Curie-Weiss law was not attempted and no other information was extracted from the data.